Nanostructure induced changes in lifetime and enhanced second-harmonic response of organic-plasmonic hybrids

Leissner, Till; Kostiuenko, Oksana; Brewer, Jonathan R.; Rubahn, Horst-Günter; Fiutowski, Jacek

Published in:
Applied Physics Letters

DOI:
10.1063/1.4938007

Publication date:
2015

Document version
Publisher's PDF, also known as Version of record

Citation for pulished version (APA):
Leißner, T., Kostiuenko, O., Brewer, J. R., Rubahn, H-G., & Fiutowski, J. (2015). Nanostructure induced changes in lifetime and enhanced second-harmonic response of organic-plasmonic hybrids. Applied Physics Letters, 107(25), 251102-(1-4). DOI: 10.1063/1.4938007

Nanostructure induced changes in lifetime and enhanced second-harmonic response of organic-plasmonic hybrids

Till Leißner, Oksana Kostiučenko, Jonathan R. Brewer, Horst-Günter Rubahn, and Jacek Fiutowski

Citation: Appl. Phys. Lett. **107**, 251102 (2015);
View online: https://doi.org/10.1063/1.4938007
View Table of Contents: http://aip.scitation.org/toc/apl/107/25
Published by the American Institute of Physics

Nanostructure induced changes in lifetime and enhanced second-harmonic response of organic-plasmonic hybrids

Till Leißner,[1,2] Oksana Kostiučenko,[1] Jonathan R. Brewer,[2] Horst-Günter Rubahn,[1] and Jacek Fiutowski[1,a)]
[1]*NanoSYD, Mads Clausen Institute, University of Southern Denmark, Alsion 2, 6400 Sønderborg, Denmark*
[2]*Department of Biochemistry and Molecular Biology, University of Southern Denmark, Campusvej 55, 5230 Odense, Denmark*

(Received 7 October 2015; accepted 3 December 2015; published online 21 December 2015)

In this letter we show that the optical response of organic nanofibers, grown from functionalized para-quaterphenylene molecules, can be controlled by forming organic-plasmonic hybrid systems. The interaction between nanofibers and supporting regular arrays of nanostructures leads to a strongly enhanced second harmonic response. At the same time, the fluorescence lifetime of the nanofibers is reduced from 0.32 ns for unstructured gold films to 0.22 ns for gold nanosquare arrays, demonstrating efficient organic–plasmonic interaction. To study the origin of these effects, we applied two-photon laser scanning microscopy and fluorescence lifetime imaging microscopy. These findings provide an effective approach for plasmon-enhanced second-harmonic generation at the nanoscale, which is attractive for nanophotonic circuitry. © *2015 AIP Publishing LLC*.
[http://dx.doi.org/10.1063/1.4938007]

Small oligomers like thiophenes or phenylenes have attracted high interest in organic opto-electronics[1] because bottom-up engineering in synthetic chemistry allows designing molecules with specific optical properties and for specific purposes.[2] Furthermore, crystalline quasi one-dimensional nano-aggregates based on these molecules can be grown with typical widths of several hundred nanometers, heights below 100 nm but lengths up to 1 mm.[3] These organic nanofibers show a multitude of optical properties, such as optical waveguiding,[4] one-dimensional random lasing,[5] anisotropic light-emission,[6,7] and second-harmonic (SH) generation.[8] Furthermore, organic nanofibers can be transferred to various receiver substrates by stamping or roll-on transfer as well as micro-manipulation, while keeping their structural and optical properties.[2] Because organic nanofibers are also capable of facilitating and controlling surface plasmon polariton (SPP) excitation and propagation,[9] they are considered as light-plasmon couplers in active plasmonic devices. The crystallinity of the fibers ensures thereby phase matching conditions and coherence of SPPs and light.[10] Hence, the use of such organic-plasmonic hybrids can be of high importance in opto-electronic engineering.

In this letter we investigate functionalized molecules, composed of a para-quaterphenyl basis unit, namely, 1-cyano-p-quaterphenylene (CNHP4). Such molecules have been grown as oriented crystals in the form of solid nanowires by a self-assembly process on muscovite mica substrates.[7,8] Due to the unsymmetrical functionalization by the cyano end group, CNHP4 molecules have a permanent molecular dipole moment. Assembled into a nanofiber, the overlay of nonlinear molecular dipoles results in a high nonlinear bulk susceptibility, as proven experimentally.[11–13]

For plasmonic circuitry applications, where the main objective is to enhance and to control the light-plasmon interaction, we transferred the CNHP4 nanofibers to lithography-defined regular arrays of gold nanosquare structures, forming an organic-plasmonic hybrid system. We expected morphological effects, in particular, local surface variations, to have a strong influence on the SH generation.[8] In particular, breaks and bends generate SH because of changes in the local dipole moment. Here, we show that SH generation can be increased significantly and in a predefined fashion by local electric field-enhancement caused by surface plasmons excited at the nanostructures. The origin of the enhanced SH signal was studied using three complementary methods, namely, two-photon laser-scanning microscopy (2P-LSM), fluorescence lifetime imaging microscopy (FLIM), and atomic force microscopy (AFM). We used 2P-LSM to map the SH generation, AFM to study morphological effects, and FLIM to confirm the strong plasmon-exciton interaction.

By these experiments we found that the SH response is enhanced significantly due to the electric field enhancement caused by surface plasmon excitation. At the same time, the fluorescence lifetime of the nanofibers is reduced because of an efficient organic–plasmonic interaction. These findings provide an effective approach for plasmon-enhanced SH generation at the nanoscale, which is attractive for nanophotonics circuitry. Furthermore, the strong plasmonic-exciton interaction might be interesting for plasmonic applications, where organic nanofibers could be exploited as active components, responsible for plasmon generation or modulation.[9,14]

CNHP4 nanofibers were grown by molecular beam epitaxy on freshly cleaved, heated muscovite mica substrates.[15] Typical dimensions vary around 100 nm in height, 300 nm in width, and 100–200 μm in length. After growth, fibers were transferred via a roll-printing technique[16] onto periodic arrays of nanosquares, with an overall array size of $100 \times 100\ \mu m^2$. The arrays were fabricated by electron beam lithography, metal/dielctric deposition, and subsequent lift-off. We studied three different

a)Electronic mail: fiutowski@mci.sdu.dk

configurations of materials: Au squares on Au film, SiO_2 squares on Au film, and Ti squares on Ti film. The squares height of 55 nm and the metal substrate thickness of 70 nm were kept for every sample. The size and the pitch distance of the nanosquares were selected to match the excitation conditions of surface plasmon polaritons by the array arrangement and a strong local field enhancement at the Au nanosquares. Therefore, the nanosquares had a size of $450 \times 450\,nm^2$ (± 10 nm), and the pitch distance was 760 ± 10 nm. The local field-enhancement and light scattering effects by the array of nanosquares are described elsewhere.[17,18] Fig. 1(a) shows a scanning electron microscopy image of the sample layout before fiber transfer. After the transfer process, the optical response of the fibers was measured. In Fig. 1(b) a bright-field micrograph is overlaid with a fluorescence microscopy image. Upon laser illumination, both SH and two-photon luminescence peaks were clearly visible in the analyzed spectrum.[19] The waveguiding properties of the nanofibers were also maintained.[19]

The SH response was mapped by a custom-built two-photon femtosecond laser scanning microscopy, based on an inverted fluorescence microscope (Nikon Eclipse TE 2000-U). The light was detected by a photomultiplier tube (Hamamatsu R585). In addition, the system was equipped with a CCD camera and a fiber spectrometer (Jaz, Ocean Optics). A broad-band Ti:Sapphire oscillator (Tsunami, Spectra Physics) providing sub 100 fs pulses at a central wavelength of 785 nm with a repetition rate of 75 MHz was used for normal sample illumination. At this photon energy the SH generation is superior to two-photon fluorescence, since the photon energy lies just below the band gap of CNHP4.[2] A sketch of the experimental setup is shown elsewhere.[20]

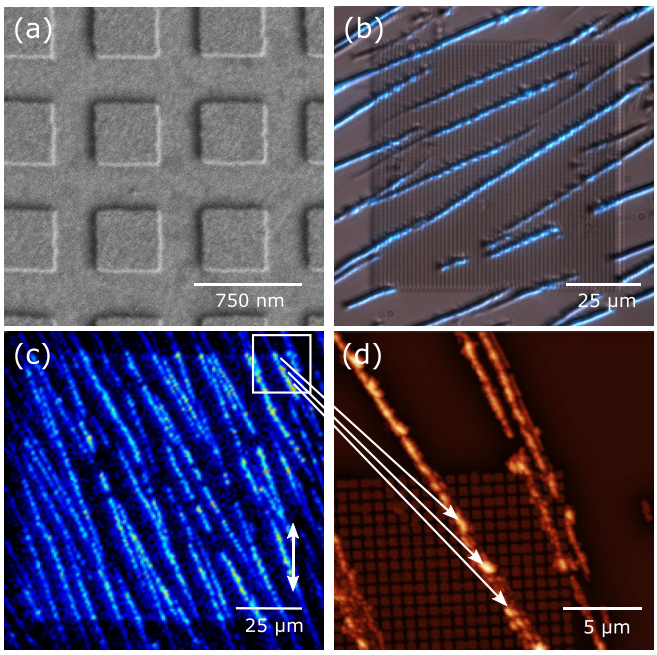

FIG. 1. (a) Scanning electron microscopy image of several nanosquares before fiber deposition; (b) Overlay of bright-field and fluorescence micrographs of a gold nanosquare array after fiber deposition; (c) Second-harmonic response of the sample upon illumination with femtosecond laser pulses at $\lambda = 790$ nm mapped by LSM. (d) AFM image from the white framed area in (c) showing the fiber morphology. The arrows indicate corresponding distinct spots in AFM and LSM images.

FLIM was conducted with another custom-built two-photon laser scanning setup, based on a Nikon Eclipse TI microscope and a Mai Tai DeepSee Ti:Sapphire laser (Spectra Physics). The repetition rate of 80 MHz and the central wavelength of 770 nm were selected to trigger fluorescence and SH signals. Lifetime images were acquired by time-correlated single-photon counting using a high speed hybrid detector (HPM-100-40, Becker & Hickl). An appropriate bandpass filter (450 ± 35 nm) was mounted in front of the detector to block the SH signal.

Fig. 1(c) shows the SH response of a CNHP4/Au hybrid system upon femtosecond illumination, mapped by LSM. The structured area is clearly visible through the significantly enhanced SH response of the nanofibers. The polarization of the incident light, represented by the arrow, has been chosen parallel to one side of the squares.

First, the SH dependence on the sample morphology was investigated. As reported earlier, the fiber surface morphology has a strong impact on the SH response, since changes in the fiber morphology lead to a strong field enhancement and further to enhanced SH generation.[8] This is confirmed in our study. In Fig. 1(d) an AFM image from the marked area in Fig. 1(c) is shown. Notably bright spots in the LSM image can be correlated to distinct spots in the AFM image. The AFM scan has been obtained after performing the optical characterization. Even though the fiber-shape is affected by the previous measurements, e.g., via material ablation, the SH enhancement is still visible in the LSM, and remains significant after many measurement scans.

To exclude pure morphological effects of the substrates, i.e., corrugation of the fibers introduced during the transfer on the structured surface, fibers from the same growth mica substrate were transferred on Ti and SiO_2 nanosquare arrays, respectively. All transfers were conducted under identical and highly controllable conditions. Fig. 2 shows laser scanning microscopy images of CNHP4 nanofibers for different receiver substrates. SH maps were again recorded during illumination with a femtosecond laser at $\lambda = 785$ nm. In Fig. 2(a), the hybrid system is formed by fibers transferred to gold nanosquares on a thin gold film, in (b) by fibers deposited on top of SiO_2 squares with a gold film underneath, and in (c) by fibers on top of titanium squares fabricated on top of a thin titanium film. The nanosquare arrays ($100 \times 100\,\mu m^2$) were located by bright-field microscopy and are marked by white squares in panels (b) and (c). In the case of gold (Fig. 2(a)), a strongly enhanced SH signal on top of the nanosquares is detected. The enhancement is absent for the other materials shown in Figs. 2(b) and 2(c). Structural inhomogeneities created during the fiber growth and transfer are similar for all samples, making the overall enhancement of the SH response of CNHP4 fibers not solely explainable by a local morphology change induced by the substrate morphology.

Further effects resulting in enhanced SH response are the lightning-rod effect and field-enhancement by surface plasmons.[21,22] The enhancement by the lightning-rod effect is based on high electric fields close to sharp metal tips, as are found at the edges of the nanosquares. Such enhancement should also be seen for the Ti squares. The enhancement

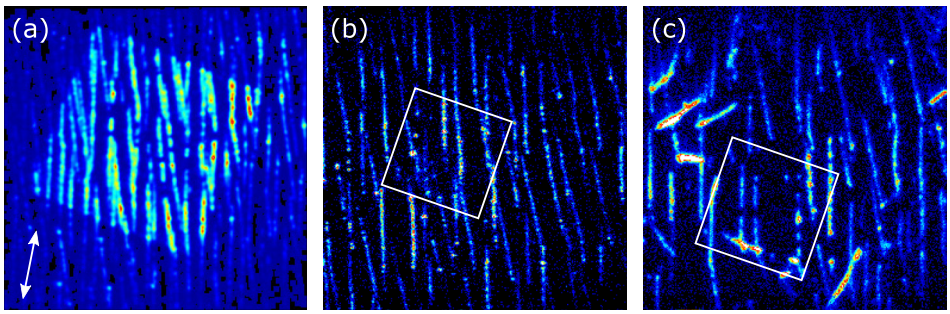

FIG. 2. SHG maps of CNHP4 nanofibers transferred to Au/Au (a), SiO_2/Au (b), and Ti/Ti (c) nanosquare arrays with an overall array size of $100 \times 100\,\mu m^2$ obtained by laser-scanning microscopy. In (a), a significantly enhanced SH signal is observed. In (b) and (c), the positions of the nanosquare arrays are marked by the white squares.

based on surface plasmons excited by the nanostructures is instead related to the dielectric function of the material. According to the material properties and the dispersion relation, the sample geometry allows the excitation of propagating surface plasmon modes only for the CNHP4/Au hybrid system.[17] Thus, our observations support the assumption that the SH response depends strongly on the local field-enhancement by surface plasmons.

Our assumption is confirmed by complementary fluorescence lifetime imaging microscopy, where fiber-plasmon interaction should open new decay channel for excitons, resulting in a reduced fluorescence lifetime. Fig. 3(a) shows a lifetime map for the gold nano-structures where the fluorescence lifetime is color-coded. The distinct reduction in lifetime τ_1 of CNHP4 fibers on top of the nanosquare array is shown by the red-green contrast. This contrast is absent for SiO_2/Au nanostructures (Fig. 3(b)) and for Ti/Ti nano-structures (Fig. 3(c)). Here, the white squares show again the positions of the structured arrays ($100 \times 100\,\mu m^2$) as found by bright-field microscopy. The arrows indicate the polarization of the light.

A closer lifetime analysis is shown in Fig. 4(a). The red curve shows the fluorescence decay of an assembly of CNHP4 nanofibers on an unstructured gold surface. The intensity decay $I(t)$ can be fitted to the model $I(t) = a_1 * \exp(-t/\tau_1) + a_2 * \exp(-t/\tau_2)$ by a two-component exponential decay using time constants τ_1 and τ_1 and amplitudes a_1 and a_2. The instrument response function was measured separately using the same experimental conditions and considered within the fitting procedure. From the fitting procedure, a fluorescence lifetime of $\tau_1 = 0.32 \pm 0.03$ns and $\tau_2 = 1.7 \pm 0.3$ns was determined. The decay is dominated by the shorter component τ_1 with relative amplitude of ca. 90%. In the vicinity of an interface, the fast component τ_1 is attributed to the non-radiative decay of CNHP4 excitons interacting with electrons in the substrate.[23] This is potentially plasmonic resonances coupling to the excitonic band structure of the molecules. The slow component τ_2 represents the intrinsic radiative decay in CNHP4 molecules and is attributed to photo-generated excitons that do not reach the fiber/substrate interface.[24]

The black curve in Fig. 4 shows the FLIM result for an assembly of CNHP4 nanofibers placed on top of a nanosquare array on the same sample. Because the number of fibers within the arbitrary chosen assembly is different, the intensities of the red and the black curves cannot be compared directly, and hence, the intensities have been normalized. However, the faster initial decay of the lifetime component τ_1 is clearly visible ($\tau_{1,\text{array}} = 0.22 \pm 0.03$ns) while τ_2 is not changed. The inset in Fig. 4 shows a histogram of lifetimes τ_1 from Fig. 3(a). Peak A corresponds to the nanostructured area, and peak B to the unstructured area. The observed width of the lifetime distribution originates among others from the spectral dependence of the lifetime[25] and from the orientation dependence of the fluorescence lifetime at interfaces.[26] Due to the latter dependency, the absolute lifetime values vary from sample to sample. However, in this report, we consider relative changes of the lifetime for the same sample, depending on whether the nanofibers have been deposited on top of the nanosquares or besides them.

In contrast to the results presented so far, nanofibers deposited on non-plasmonic materials, i.e., SiO_2/Au and Ti/Ti substrates, show no shortened lifetime on top of the squares, neither in the fast nor in the slow decay component. Lifetime values for SiO_2 (Ti) are $\tau_1 = 0.40$ns (0.31 ns) and $\tau_2 = 1.94$ns (1.59 ns). Lifetime maps of the τ_2 are shown in the supplementary material.[19]

These observations give clear evidence that the observed lifetime reduction for CNHP4 nanofibers transferred to gold nanostructures can be explained by a strong nanofiber–plasmon interaction.

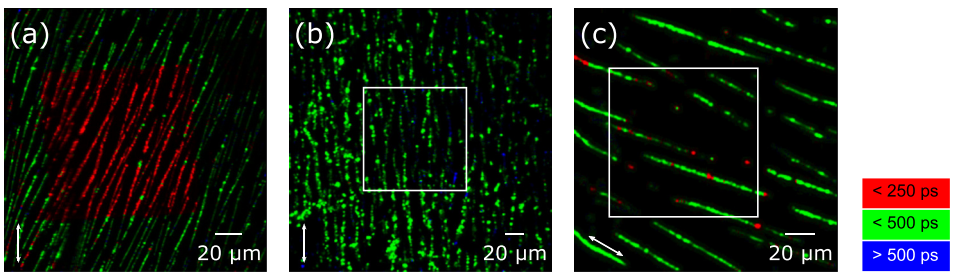

FIG. 3. Fluorescence lifetime maps for different substrate and nanosquare materials: (a) Au squares on Au film; (b) SiO_2 squares on Au film; and (c) Ti squares on Ti film. The fast lifetime component τ_1 of the two component exponential decay is encoded in the discrete color scale shown at the right. For Au, the fast lifetime decay component τ_1 exhibits a significant red-green contrast between structured and unstructured areas. For SiO_2/Au and Ti/Ti substrates no lifetime contrast is observed. The nanosquare arrays were located by additional bright-field microscopy and are marked by white squares.

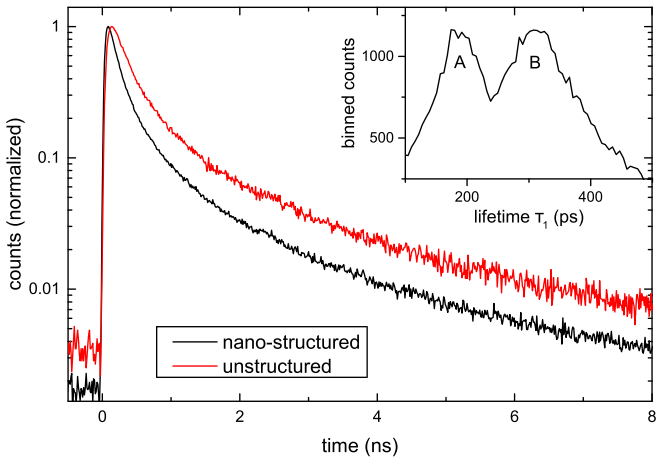

FIG. 4. Two-photon fluorescence lifetime decay for an assembly of CNHP4 nanofibers placed on top of gold nanosquares (black) and on unstructured areas (red). The inset shows a lifetime histogram. Peak A shows the typical lifetime on gold nanosquares, and peak B the typical lifetime on unstructured areas.

In this letter we have shown that organic-plasmonic hybrids are capable of enhancing non-linear effects in nanofibers. In detail we studied SH generation in organic CNHP4 nanofibers. We could show that by transferring these fibers to properly designed substrates the SH response can be enhanced significantly. We could further show that mainly surface plasmons play a crucial role in tuning the SH response. In the case of the investigated organic-plasmonic hybrid system, the local field enhancement is superior to the morphological and lightning-rod effects. The reduced fluorescence lifetime for fibers transferred to nano-structured areas emphasizes the importance of organic-plasmonic coupling.

Amplifying the non-linear response of organic nanofibers by tuning the local electric field of the receiver substrate will play an important role in the development of organic opto-electronic devices due to a strong demand for active components that can convert optical signals into plasmonic signals and vice versa.[13] The high degree of flexibility in tuning structural and optical properties make phenylene-based nanofibers a very attractive component which is attractive for nanophotonic circuitry.

The authors thank Arne Lützen from Bonn University for providing CNHP4 molecules and Francesco Quochi from University of Cagliari for fruitful discussions. Financial funding of this work was provided by the Danish Council for Independent Research (FTP-project No. 09-072949 ANAP) and by the SDU2020 fund.

[1]M. Muccini, Nat. Mater. **5**, 605 (2006).
[2]J. Kjelstrup-Hansen, C. Simbrunner, and H.-G. Rubahn, Rep. Prog. Phys. **76**, 126502 (2013).
[3]L. Kankate, F. Balzer, H. Niehus, and H.-G. Rubahn, Thin Solid Films **518**, 130 (2009).
[4]F. Balzer, V. Bordo, A. Simonsen, and H.-G. Rubahn, Phys. Rev. B **67**, 115408 (2003).
[5]F. Quochi, F. Cordella, A. Mura, G. Bongiovanni, F. Balzer, and H.-G. Rubahn, J. Phys. Chem. B **109**, 21690 (2005).
[6]J. Brewer and H.-G. Rubahn, Phys. Status Solidi C **2**, 4058 (2005).
[7]M. Schiek, F. Balzer, K. Al-Shamery, A. Lützen, and H.-G. Rubahn, Soft Matter **4**, 277 (2008).
[8]J. Brewer, M. Schiek, A. Lützen, K. Al-Shamery, and H.-G. G. Rubahn, Nano Lett. **6**, 2656 (2006).
[9]T. Leißner, C. Lemke, J. Fiutowski, J. W. Radke, A. Klick, L. Tavares, J. Kjelstrup-Hansen, H.-G. Rubahn, and M. Bauer, Phys. Rev. Lett. **111**, 046802 (2013).
[10]E. Skovsen, T. Søndergaard, J. Fiutowski, P. Simesen, A. Osadnik, A. Lützen, H.-G. Rubahn, S. I. Bozhevolnyi, and K. Pedersen, Opt. Express **20**, 16715 (2012).
[11]J. Brewer, M. Schiek, and H.-G. Rubahn, Opt. Commun. **283**, 1514 (2010).
[12]K. Pedersen, M. Schiek, J. Rafaelsen, and H. G. Rubahn, Appl. Phys. B: Lasers and Optics **96**, 821 (2009).
[13]P. Simesen, T. Søndergaard, E. Skovsen, J. Fiutowski, H.-G. Rubahn, S. I. Bozhevolnyi, and K. Pedersen, Opt. Express **23**, 16356 (2015).
[14]T. W. Ebbesen, C. Genet, and S. I. Bozhevolnyi, Phys. Today **61**(5), 44 (2008).
[15]J. Brewer, M. Schiek, I. Wallmann, and H.-G. Rubahn, Opt. Commun. **281**, 3892 (2008).
[16]L. Tavares, J. Kjelstrup-Hansen, and H.-G. Rubahn, Small **7**, 2460 (2011).
[17]A. Hohenau, J. R. Krenn, F. J. Garcia-Vidal, S. G. Rodrigo, L. Martin-Moreno, J. Beermann, and S. I. Bozhevolnyi, Phys. Rev. B **75**, 85104 (2007).
[18]J. Fiutowski, C. Maibohm, J. Kjelstrup-Hansen, and H. G. Rubahn, Appl. Phys. Lett. **98**, 193117 (2011).
[19]See supplementary material at http://dx.doi.org/10.1063/1.4938007 for optical properties of CNHP4 nanofibers deposited on gold nanosquare arrays as well as for lifetime maps of decay component τ_2.
[20]J. Fiutowski, C. Maibohm, O. Kostiučenko, J. Kjelstrup-Hansen, and H.-G. Rubahn, J. Nanophotonics **6**, 063515 (2012).
[21]M. I. Stockman, Phys. Today **64**(2), 39 (2011).
[22]L. Novotny and S. J. Stranick, Annu. Rev. Phys. Chem. **57**, 303 (2006).
[23]T. D. Neal, K. Okamoto, A. Scherer, M. S. Liu, and A. K.-Y. Jen, Appl. Phys. Lett. **89**, 221106 (2006).
[24]L. Tavares, M. Cadelano, F. Quochi, C. Simbrunner, G. Schwabegger, M. Saba, A. Mura, G. Bongiovanni, D. A. da Silva Filho, W. F. da Cunha, H.-G. Rubahn, and J. Kjelstrup-Hansen, J. Phys. Chem. C **119**, 15689 (2015).
[25]J. R. Garcia, M. H. Gehlen, H. P. M. de Oliveira, and F. C. Nart, J. Braz. Chem. Soc. **19**, 1306 (2008).
[26]M. Kreiter, M. Prummer, B. Hecht, and U. P. Wild, J. Chem. Phys. **117**, 9430 (2002).